



Published in final edited form as:

*Biotechnol Prog.* 2011 ; 27(3): 863–869. doi:10.1002/btpr.604.

## Immobilization of Active Human Carboxylesterase 1 in Biomimetic Silica Nanoparticles

Jonathan S. Edwards<sup>1</sup>, Amar Kumbhar<sup>2</sup>, Adam Roberts<sup>1</sup>, Andrew C. Hemmert<sup>1</sup>, Carol C. Edwards<sup>3</sup>, Philip M. Potter<sup>3</sup>, and Matthew R. Redinbo<sup>1,4,\*</sup>

<sup>1</sup>Department of Biochemistry and Biophysics, University of North Carolina at Chapel Hill, Chapel Hill, NC

<sup>2</sup>Chapel Hill Analytical and Nanofabrication Laboratory, University of North Carolina at Chapel Hill, Chapel Hill, North Carolina

<sup>3</sup>Department of Chemical Biology and Therapeutics, St. Jude Children's Research Hospital, Memphis, TN

<sup>4</sup>Department of Chemistry, University of North Carolina at Chapel Hill, Chapel Hill, NC

### Abstract

The encapsulation of proteins in biomimetic silica has recently been shown to successfully maintain enzymes in their active state. Organophosphate (OP) compounds are employed as pesticides as well as potent chemical warfare nerve agents. Because these toxicants are life threatening, we sought to generate biomimetic silicas capable of responding to OPs. Here, we present the silica encapsulation of human drug metabolism enzyme carboxylesterase 1 (hCE1) in the presence of a range of catalysts. hCE1 was successfully encapsulated into silica particles when lysozyme or the peptide R5 were used as catalysts; in contrast, polyethyleneimine (PEI), a catalyst employed to encapsulate other enzymes, did not facilitate hCE1 entrapment. hCE1 silica particles in a column chromatography format respond to the presence of the organophosphate (OP) pesticides paraoxon and dimethyl-p-nitrophenyl phosphate in solution. These results may lead to novel approaches to detect OP pesticides or other weaponized agents that bind hCE1.

### Keywords

drug metabolism; biomimetic silica; enzyme immobilization; organophosphate pesticide

## INTRODUCTION

Sol-gel and biomimetic reactions have facilitated the use of immobilized enzymes in a range of applications<sup>1</sup>. For example, several recent studies have employed the biomineralization of silica to encapsulate a variety of enzymes. This reaction occurs rapidly at room temperature using tetramethylorthosilicate (TMOS) and a polycationic catalyst to promote silica formation around the target enzyme. Proteins encapsulated using this approach can be used to catalyze highly specific reactions, to screen for enzyme inhibitors, or to detect the presence of chemical compounds. Indeed, silica particles containing enzymes have been employed in biosensing applications, including microfluidic devices and aerosol detectors<sup>2,3</sup>.

\*Corresponding Author: Matthew R. Redinbo, Ph.D. Department of Chemistry University of North Carolina at Chapel Hill Chapel Hill, NC 27599-3290 (919) 843-8910; (919) 962-2388 fax redinbo@unc.edu.

There are several advantages to using silica particles for encapsulation, including the fact that the mild reaction conditions promote the capture of active enzymes, and, in some cases, increase enzyme stability<sup>4</sup>. The simplicity and speed of the reaction also allow for rapid encapsulation and the cost-effective production of the particles for various needs. For example, encapsulated enzymes could be used in a column format to monitor for chemical contaminants in water sources. However, encapsulation efficiency varies with the catalyst-enzyme pair<sup>5</sup>. Thus, optimal encapsulation conditions must be identified for each enzyme before they can be applied in a useful setting.

One promising application of encapsulated protein is the detection of chemical compounds, such as organophosphates (OP). OPs are employed as agricultural pesticides, but have also been weaponized for use as highly toxic nerve agents like sarin, soman, and cyclosarin<sup>6,7</sup>. OP toxicity arises from the noncompetitive inhibition of acetylcholinesterase (AChE), which produces sustained acetylcholine stimulus of the muscarinic and nicotinic receptors and may lead to diaphragm incapacitation resulting in suffocation. Biosensors containing enzymes inhibited by OPs have recently been explored for military and civilian applications<sup>2,8,9</sup>.

The human liver carboxylesterase 1 (hCE1) is a promiscuous serine hydrolase that catalyzes the hydrolysis of endogenous molecules and xenobiotics containing ester, amide, or thioester bonds<sup>10,11,12,13,14,15,16,17</sup>. This structural AChE homolog is currently being explored as a prophylactic bioscavenger to decontaminate OP toxicity<sup>18</sup>. Based upon the ability of hCE1 to bind Ops<sup>15,18</sup>, we sought to examine the silica encapsulation of hCE1 and the ability of the resultant nanoparticles to detect the presence of OP toxicants.

## MATERIALS AND METHODS

### Expression and purification of hCE1

A secreted form of hCE1 was expressed using baculovirus infection of *Spodoptera frugiperda* Sf21 cells and purified as described<sup>19</sup>. hCE1 was concentrated in 50 mM HEPES (pH 7.4) and stored at 4 °C. Protein concentration was determined spectrophotometrically using an extinction coefficient 17700 M<sup>-1</sup> cm<sup>-1</sup> (NanoDrop, ND-1000 Spectrophotometer).

### Preparation of silica nanoparticles with hCE1

All materials were purchased from Sigma-Aldrich unless otherwise noted. A stock solution of lysozyme at 100 mg/ml was prepared in 0.1 M potassium phosphate buffer (pH 7.4). A solution of hydrolyzed tetramethyl orthosilicate (TMOS) was freshly prepared by diluting into 1 mM hydrochloric acid to a final concentration of 1 M. A typical reaction mixture consisted of 800  $\mu$ l of 0.1 M potassium phosphate buffer containing 5  $\mu$ g of hCE1, 100  $\mu$ l of lysozyme or R5 solution (100 mg/ml), and 100  $\mu$ l of 1 M hydrolyzed TMOS. The mixture was incubated at room temperature (22 °C) for 10 minutes with gentle shaking. The slurry was centrifuged for 60 s (13,000 rpm) to remove the particles and washed in ddH<sub>2</sub>O three times. Control particles were produced in a similar manner using a reaction mixture without hCE1 by combining 800  $\mu$ l of 0.1 M potassium phosphate buffer, 100  $\mu$ l of lysozyme solution, and 100  $\mu$ l of hydrolyzed TMOS. Combination particles were created using ratios of polyethyleneimine (1%) to lysozyme (100 mg/mL) 1:4, 1:1, 4:1 as the catalyst to compare the efficiency of enzyme incorporation. The total volume of catalyst used was always equal to 10% of the silica reaction.

### Scanning and transmission electron microscopy

The morphology of silica-encapsulated hCE1 with various catalyst was observed with a Hitachi 4700 Scanning Electron Microscope (SEM) and a JEOL 2010F Transmission Electron Microscope (TEM). SEM samples were prepared by depositing dry powdered

samples on a double-stick carbon tape on an aluminium SEM sample holder. The samples were coated with a 3nm Au-Pd conductive coating in order to prevent charging effect during imaging. TEM samples were prepared by air-drying a drop of concentrated reaction mixture on a carbon-stabilized copper grid (Ted Pella Inc.).

### Determination of hCE1 enzyme activity

Activity of silica-encapsulated or solution hCE1 were monitored using para-nitrophenyl butyrate (pNPB) as a substrate and measuring the absorbance of the para-nitrophenol product at 410 nm using a Pherastar spectrophotometer (BMG Labtech). The substrate was dissolved in ethanol to a concentration of 1 M, and then diluted to 10 mM in 0.1 M phosphate buffer pH 7.4. hCE1 silica particles were mixed with substrate at a final concentration of 5 mM. Supernatants from the washes were saved and monitored in the same fashion to determine the incorporation efficiency of the silica reactions.

### Kinetics of para-nitrophenyl butyrate hydrolysis

$K_m$ ,  $V_{max}$ , and  $k_{cat}$  values were determined by monitoring the conversion of pNPB to para-nitrophenol at 410 nm using a Pherastar spectrophotometer (BMG Labtech). Substrate was prepared as described above. Data was collected over 4 minutes and the linear portions were used for the linear regressions to calculate the reaction velocities. Kinetic parameters were determined by plotting the reaction velocities versus substrate concentration. An extinction coefficient of 17700 was used for para-nitrophenol in calculating the  $V_{max}$ . The molecular weight for hCE1 that was used to calculate the  $k_{cat}$  was 61.68 kDa. The Prism software packaged was used to fit the data (GraphPad, San Diego, CA).

### Column-based experiments

Column activity of silica-encapsulated hCE1 was determined using a stainless steel microbore column (2 cm × 2 mm, Upchurch Scientific, Oak Harbor, WA) with 0.5 μm frits. The silica nanoparticle reaction mixture was scaled up to a total of 10 mL. The particles were resuspended in 0.1 M phosphate buffer pH 7.4 and pumped at a flow rate of 10 μL/min to pack the column. The column was washed with 10 column volumes of phosphate buffer prior to use. All column experiments were performed at room temperature (22 °C) at a flow rate of 100 μL/min using a NE-1000 syringe pump (New Era Pump Systems, Wantagh, NY). Phosphate buffer containing 5 mM substrate was flowed through the column. Samples were collected and analyzed in a Pherastar spectrophotometer to measure absorbance at 410 nm until the substrate hydrolysis had reached a maximum.

### Organophosphate pesticide detection

Using a column constructed in the manner described above, phosphate buffer containing 5 mM substrate was applied and absorbance was measured until the substrate hydrolysis reached its maximum value. Phosphate buffer containing 5 mM substrate and paraoxon or DMPNPP (1mM) was then flowed through the column, and absorbance was measured at 410 nm to determine if OP was detected. A drop in absorbance at 410 nm correlates with enzyme inhibition because the product of the enzyme assay, paranitrophenol, absorbs at 410 nm. The pesticides were diluted 1:10 in methanol and further diluted in 0.1 M phosphate buffer pH 7.4 to their final concentration. Inhibition was confirmed by flowing phosphate buffer containing 5 mM substrate through the column and monitoring absorbance at 410 nm.

## RESULTS

### Silica Encapsulation of Active hCE1

Initial experiments employed lysozyme as the polycation catalyst for silica nanoparticle formation in reaction conditions containing hydrolyzed tetramethylorthosilicate (TMOS), lysozyme (100 mg/mL), and potassium phosphate buffer at pH 7.4 with 5  $\mu\text{g}$  of hCE1 enzyme. hCE1 was incorporated into the particles with high efficiency, leaving no enzyme activity in the supernatant (Figure 1A). In addition, no hCE1 activity was detected in solutions used to wash the particles after formation (Figure 1A). Thus, while the process may render some hCE1 inactive, all detectable enzyme activity localized solely to the particles. hCE1 activity in the silica nanoparticles, as measured by para-nitrophenyl butyrate (pNPB) hydrolysis, reached the same maximal velocity as 5  $\mu\text{g}$  of hCE1 in solution; however, the encapsulated enzyme exhibited a slightly reduced initial rate of product formation (Figure 1A, Table I). Multiple washes of silica particles with phosphate buffer did not release active enzyme, indicating that the hCE1 activity associated with the particles did not arise from enzyme adhered relatively loosely to particle surfaces. Similarly, several washes of particles in 1% Tween 20 did not dissociate hCE1 activity from the particles (data not shown). When washed in detergent, the hCE1 activity in the particles was comparable to the activity measured from particles washed in buffer alone (Table I).

We examined the effect of entrapping hCE1 in silica on the enzyme's ability to hydrolyze pNPB. Kinetic experiments were performed maintaining a constant amount of enzyme with varied substrate concentrations to determine initial reaction velocities. Michaelis-Menten kinetics was assumed and the kinetic parameters were determined (Table II). hCE1 in silica had a  $K_m$  that was approximately three times higher than enzyme in solution. Furthermore, hCE1 in silica exhibited a slightly reduced efficiency ( $k_{\text{cat}}/K_m = 3.1 \times 10^4 \text{ s}^{-1} \text{ M}^{-1}$ ) relative to free enzyme ( $k_{\text{cat}}/K_m = 1.9 \times 10^4 \text{ s}^{-1} \text{ M}^{-1}$ ). These solution values are in agreement with previously reported kinetic parameters for hCE1 with para-nitrophenyl butyrate (pNPB)<sup>20</sup>. Taken together, these results demonstrate that active hCE1 can be efficiently incorporated into lysozyme-catalyzed silica nanoparticles.

We also investigated the ability of other cationic catalysts to generate hCE1-encapsulated silica nanoparticles. We created silica particles in the presence of hCE1 using the following catalysts: cationic peptide R5 ( $\text{NH}_2\text{-SSKKS GSYSGSKGSKRRIL-CO}_2\text{H}$ )<sup>21</sup> and the polymer polyethyleneimine (PEI). We found that silica particles formed with the R5 peptide exhibited similar incorporation efficiency and enzyme activity as the lysozyme hCE1-silica particles (Figure 1B, Table I). In contrast, PEI catalyzed particles, which formed immediately upon mixing (compared to ~5 minutes with the lysozyme or R5 silica particles) excluded hCE1 into the supernatant and thus had no associated enzyme activity with the particles. (Figure 1C; Table I).

We hypothesized that the lack of entrapped hCE1 during PEI-mediated particle creation was caused by either the rapid particle formation or catalyst size. That hypothesis was tested by creating beads using different ratios of lysozyme and PEI in the presence of the same amount of hCE1 (80% lysozyme:20% PEI, 50% lysozyme:50% PEI, and 20% lysozyme:80% PEI). It was determined that increasing the amount of lysozyme relative to PEI improved the encapsulation of hCE1, but that no silica particles formed in the presence of PEI exhibited higher levels of entrapped hCE1 activity than those formed without PEI (Figures 1D–F, Table I). We also concluded that hCE1 alone could not facilitate the precipitation of silica particles without either lysozyme or the R5 peptide (data not shown). The reaction was cooled to 4°C to see if the silica condensation could be slowed in the presence of PEI. The reaction appeared to occur just as fast and no hCE1 was incorporated into the particles (data not shown). Thus, we conclude that macromolecular catalysts as small as the R5 peptide and

as large as hen egg white lysozyme are capable of generating silica nanoparticles that entrap active hCE1.

### Electron Microscopy of hCE1 Nanoparticles

We employed scanning electron microscopy (SEM) and transmission electron microscopy (TEM) to examine the size and morphology of silica particles produced in the presence of hCE1. Silica hCE1 particles using lysozyme as the catalyst were larger than the particles obtained using either R5 or PEI as catalysts. Lysozyme-catalyzed particles were 0.8–1  $\mu\text{m}$  in diameter and appeared to fuse to form large aggregates on the order of  $\sim 2 \mu\text{m}$  (Figure 2A). In contrast, silica particles obtained in the presence of hCE1 using R5 and PEI as catalysts formed individual particles 0.3–0.8  $\mu\text{m}$  in diameter and an aggregate size of  $\sim 1 \mu\text{m}$  (Figure 2B and C). Dynamic light scattering (DLS) performed on the lysozyme catalyzed silica particles confirmed the sizes measured from SEM analysis (data not shown). The silica particles formed using the combinations of lysozyme and PEI were smaller ( $\sim 0.5 \mu\text{m}$ ) and appear monodisperse as compared to the particles using only lysozyme or PEI as catalysts (Figure 2 D, E, F). Increasing amounts of PEI in the reaction lead to the formation of smaller particles and smaller aggregate size.

TEM images corroborated the SEM data (Figure 3 A, B). For example, particles obtained in the presence of lysozyme were larger in size compared to that of the PEI-catalyzed silica particles. Further, the TEM images revealed that the lysozyme-catalyzed silica particles exhibited a smoother surface than that of the PEI-catalyzed particles. In contrast, the particles obtained using ratios of lysozyme and PEI as catalysts, appeared to have rougher surface features similar to that seen for the PEI catalyzed particles. This was presumably due to the presence of PEI on the particle surface (Figure 3 C, D and E).

### Solution Detection Studies of Pesticides with hCE1 Nanoparticles

We examined whether silica nanoparticles containing active hCE1 could function in a column chromatography format. Biosilica particles formed with lysozyme and hCE1 (see Figures 1A, 2A) were packed using buffer flowed into a stainless steel microbore column (2 cm  $\times$  2 mm) with 0.5  $\mu\text{m}$  frits controlled by a New Era single syringe pump (New Era Pump Systems, Wantagh, NY). Particles catalyzed with lysozyme in the presence of hCE1 were chosen because they were cost-effective and displayed robust entrapment efficiency and enzyme activity. After extensive washing of the column, 5 mM pNPB was applied to the column and para-nitrophenol formation was observed, indicating that hCE1 retains its enzyme activity in the silica particles packed within the column (Figure 4). No hCE1 activity was detected in the solutions used to wash the column, supporting the conclusion that the enzyme remained encapsulated in the column particles.

To determine whether columns containing hCE1 biosilica nanoparticles were capable of detecting organophosphate pesticides, we added the pesticides and monitored substrate conversion to para-nitrophenol. Columns were operated in the manner described above, and equilibrated such that a stable amount of para-nitrophenol product was being formed over time (e.g. 10  $\mu\text{mol}/\text{min}$ ). At that point, 1 mM diethyl para-nitrophenyl phosphate (paraoxon) was applied to a column, which produced a dramatic drop in enzyme activity resulting in decreased substrate conversion (Figure 4A). Detection of this hCE1 inhibitor occurs rapidly, likely due to the small column volume of 16.2  $\mu\text{L}$ . hCE1 remains permanently inhibited by paraoxon even 50 minutes ( $\sim 70$  column volumes) after this inhibitor is removed from the substrate-containing solution applied to the column (Figure 4A). In a second study, dimethyl-*para*-nitrophenylphosphate (DMPNPP) was applied to a column instead of paraoxon. In this case, detection of the hCE1 inhibitor was rapid, but once the inhibitor was removed, hCE1 activity returned over time (Figure 4B).

Paraoxon inhibits hCE1 activity 3-fold more robustly in solution than DMPNPP (with bimolecular rates of inhibition  $[k_i]$  values of  $9.1 \pm 0.5 \times 10^6 \text{ min}^{-1}\text{M}^{-1}$  and  $2.9 \pm 0.3 \times 10^6 \text{ min}^{-1}\text{M}^{-1}$ , respectively)<sup>18</sup>. Taken together, these results indicate that OP pesticides can be detected using hCE1 biosilica nanoparticles within a column chromatography format.

## DISCUSSION

Silica nanoparticles have the potential to generate a range of platforms for biodetection. We have shown that hCE1 can be effectively encapsulated into silica nanoparticles catalyzed by lysozyme, and that these particles maintain overall enzyme activity comparable to hCE1 in solution. In our studies, however, lysozyme-encapsulated hCE1 exhibited a slightly reduced initial rate of product formation, although activity reached that of free hCE1 over time. We hypothesize that this effect is caused by impeded substrate access to the active site of the enzyme in the silica matrix. We also found that hCE1 is more efficiently incorporated into silica nanoparticles using lysozyme as a catalyst in comparison to PEI catalyzed silica particles. Similar results have been observed with other enzymes during encapsulation<sup>5</sup>.

We focused on three catalysts – lysozyme, the R5 peptide, and PEI – which have been demonstrated to be successful in previous studies with other target enzymes<sup>22,23,24</sup>. Based on our results, we hypothesize that the lack of entrapped hCE1 during PEI-mediated particle creation was caused by the rapid particle formation and the small size of PEI. For example, when lysozyme was used as a catalyst, the reaction proceeded slowly taking approximately 2 minutes until particles can be visualized in solution; in contrast, when PEI was employed, the particles formed immediately. This observation, combined with the smaller sized PEI-catalyzed particles relative to those created with lysozyme suggested that PEI-generated silica matrixes excluded hCE1 under the reaction conditions employed. The lysozyme-catalyzed particles underwent more complete condensation similar to that seen for pure sol-gel silica reactions with other enzymes<sup>25</sup>.

Finally, we demonstrated that silica nanoparticles containing hCE1 are able to detect OP pesticides in a column chromatography format. The drop in hCE1 activity correlated with the strength of the inhibitor employed; for example, paraoxon, a more potent hCE1 inhibitor, did not allow enzyme activity to recover during the time course of the study. It is possible that such an apparatus could be employed in the detection of OP pesticides or chemical weapons agents using silica nanoparticles containing hCE1. Both liquid- and gas-based detection have already been reported involving other enzymes, including the cholinesterases<sup>2</sup>. Our data indicate that another member of the serine hydrolase family of enzymes may also be employed for this or related technologies.

## Acknowledgments

This work was supported in part by NIH Grants NS58089, CA108775, DA018116, an NIH Cancer Center Core Grant CA21765, and by the American Lebanese Syrian Associated Charities (ALSAC) and St. Jude Children's Research Hospital (SJCRH)

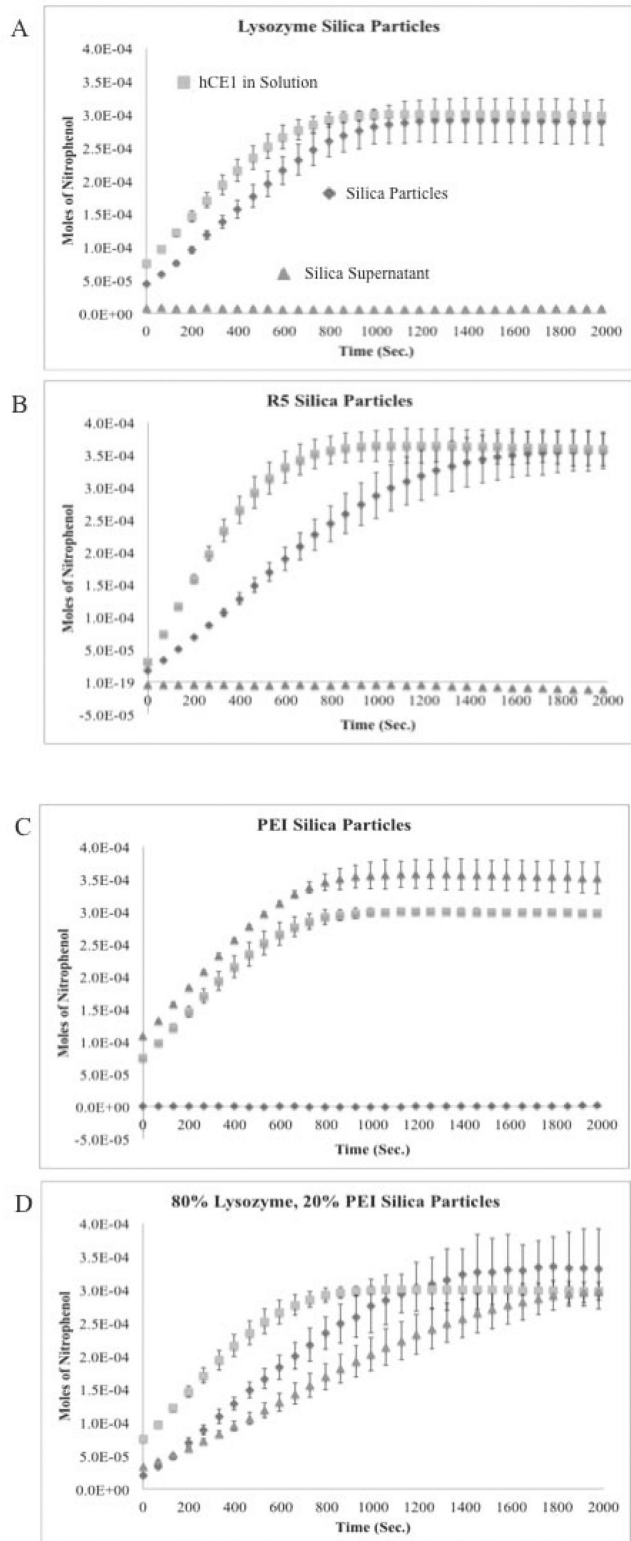
## REFERENCES

1. Avnir D, Coradin T, Lev O, Livage J. Recent bio-applications of sol-gel materials. *J of Mat Chem.* 2006; 16(11):1013–1030.
2. Luckarift HR, Greenwald R, Bergin MH, Spain JC, Johnson GR. Biosensor system for continuous monitoring of organophosphate aerosols. *Biosens Bioelectron.* 2007; 23(3):400–6. [PubMed: 17582755]
3. Luckarift HR, Ku BS, Dordick JS, Spain JC. Silica-immobilized enzymes for multi-step synthesis in microfluidic devices. *Biotechnol Bioeng.* 2007; 98(3):701–5. [PubMed: 17415802]

4. Luckarift HR, Spain JC, Naik RR, Stone MO. Enzyme immobilization in a biomimetic silica support. *Nat Biotechnol.* 2004; 22(2):211–3. [PubMed: 14716316]
5. Betancor L, Luckarift HR. Bioinspired enzyme encapsulation for biocatalysis. *Trends Biotechnol.* 2008; 26(10):566–72. [PubMed: 18757108]
6. Aardema H, Meertens JH, Ligtenberg JJ, Peters-Polman OM, Tulleken JE, Zijlstra JG. Organophosphorus pesticide poisoning: cases and developments. *Neth J Med.* 2008; 66(4):149–53. [PubMed: 18424861]
7. Newmark J. Nerve agents. *Neurologist.* 2007; 13(1):20–32. [PubMed: 17215724]
8. Luckarift HR, Johnson GR, Spain JC. Silica-immobilized enzyme reactors; application to cholinesterase-inhibition studies. *J Chromatogr B Analyt Technol Biomed Life Sci.* 2006; 843(2): 310–6.
9. Ramanathan M, Luckarift HR, Sarsenova A, Wild JR, Ramanculov EK, Olsen EV, Simonian AL. Lysozyme-mediated formation of protein-silica nano-composites for biosensing applications. *Colloids Surf B Biointerfaces.* 2009; 73(1):58–64. [PubMed: 19481427]
10. Bencharit S, Edwards CC, Morton CL, Howard-Williams EL, Kuhn P, Potter PM, Redinbo MR. Multisite promiscuity in the processing of endogenous substrates by human carboxylesterase 1. *J Mol Biol.* 2006; 363(1):201–14. [PubMed: 16962139]
11. Bencharit S, Morton CL, Howard-Williams EL, Danks MK, Potter PM, Redinbo MR. Structural insights into CPT-11 activation by mammalian carboxylesterases. *Nat Struct Biol.* 2002; 9(5):337–42. [PubMed: 11967565]
12. Bencharit S, Morton CL, Hyatt JL, Kuhn P, Danks MK, Potter PM, Redinbo MR. Crystal structure of human carboxylesterase 1 complexed with the Alzheimer's drug tacrine: from binding promiscuity to selective inhibition. *Chem Biol.* 2003; 10(4):341–9. [PubMed: 12725862]
13. Bencharit S, Morton CL, Xue Y, Potter PM, Redinbo MR. Structural basis of heroin and cocaine metabolism by a promiscuous human drug-processing enzyme. *Nat Struct Biol.* 2003; 10(5):349–56. [PubMed: 12679808]
14. Fleming CD, Bencharit S, Edwards CC, Hyatt JL, Tsurkan L, Bai F, Fraga C, Morton CL, Howard-Williams EL, Potter PM. Structural insights into drug processing by human carboxylesterase 1: tamoxifen, mevastatin, and inhibition by benzil. *J Mol Biol.* 2005; 352(1):165–77. others. [PubMed: 16081098]
15. Fleming CD, Edwards CC, Kirby SD, Maxwell DM, Potter PM, Cerasoli DM, Redinbo MR. Crystal structures of human carboxylesterase 1 in covalent complexes with the chemical warfare agents soman and tabun. *Biochemistry.* 2007; 46(17):5063–71. [PubMed: 17407327]
16. Redinbo MR, Bencharit S, Potter PM. Human carboxylesterase 1: from drug metabolism to drug discovery. *Biochem Soc Trans.* 2003; 31(Pt 3):620–4. [PubMed: 12773168]
17. Redinbo MR, Potter PM. Mammalian carboxylesterases: from drug targets to protein therapeutics. *Drug Discov Today.* 2005; 10(5):313–25. [PubMed: 15749280]
18. Hemmert AC, Otto TC, Wierdl M, Edwards CC, Fleming CD, MacDonald M, Cashman JR, Potter PM, Cerasoli DM, Redinbo MR. Human carboxylesterase 1 stereoselectively binds the nerve agent cyclosarin and spontaneously hydrolyzes the nerve agent sarin. *Mol Pharmacol.* 2010; 77(4):508–16. [PubMed: 20051531]
19. Morton CL, Potter PM. Comparison of *Escherichia coli*, *Saccharomyces cerevisiae*, *Pichia pastoris*, *Spodoptera frugiperda*, and COS7 cells for recombinant gene expression. Application to a rabbit liver carboxylesterase. *Mol Biotechnol.* 2000; 16(3):193–202. [PubMed: 11252804]
20. Wadkins RM, Morton CL, Weeks JK, Oliver L, Wierdl M, Danks MK, Potter PM. Structural constraints affect the metabolism of 7-ethyl-10-[4-(1-piperidino)-1-piperidino]carbonyloxycamptothecin (CPT-11) by carboxylesterases. *Mol Pharmacol.* 2001; 60(2): 355–62. [PubMed: 11455023]
21. Nam DH, Won K, Kim YH, Sang BI. A novel route for immobilization of proteins to silica particles incorporating silaffin domains. *Biotechnol Prog.* 2009; 25(6):1643–9. [PubMed: 19774662]
22. Betancor L, Berne C, Luckarift HR, Spain JC. Coimmobilization of a redox enzyme and a cofactor regeneration system. *Chem Commun (Camb).* 2006; (34):3640–2. [PubMed: 17047791]

23. Luckarift HR, Dickerson MB, Sandhage KH, Spain JC. Rapid, room-temperature synthesis of antibacterial bionanocomposites of lysozyme with amorphous silica or titania. *Small*. 2006; 2(5): 640–3. [PubMed: 17193101]
24. Naik RR, Tomczak MM, Luckarift HR, Spain JC, Stone MO. Entrapment of enzymes and nanoparticles using biomimetically synthesized silica. *Chem Commun (Camb)*. 2004; (15):1684–5. [PubMed: 15278136]
25. Gao Y, Heinemann A, Knott R, Bartlett J. Encapsulation of protein in silica matrices: structural evolution on the molecular and nanoscales. *Langmuir*. 2010; 26(2):1239–46. [PubMed: 19722605]





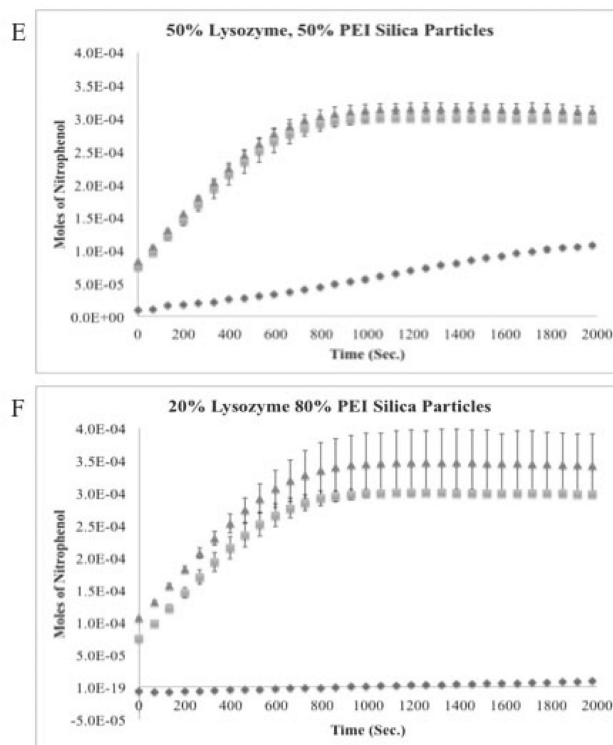


**Figure 1.**

Activity assays measuring the formation of para-nitrophenol at 410 nm. Silica particles were formed using the respective catalysts and the absorbance was measured over time. Activity was measured for the silica particles and the supernatant from the reaction, then compared to hCE1 in solution. All data points had an N = 3 and S.E. is reported.

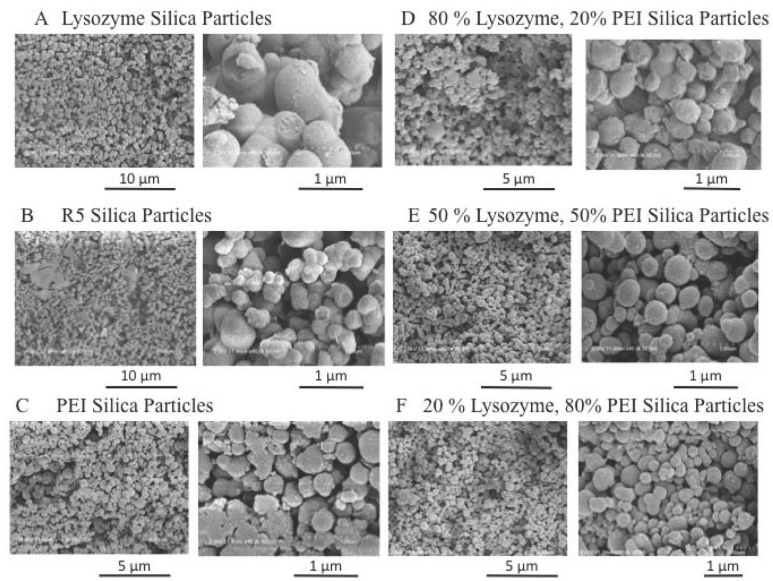


**Figure 2.** SEM images of the silica particles containing hCE1 at two magnifications. The samples were sputtered with Au-Pd conductive coating prior to analyses.

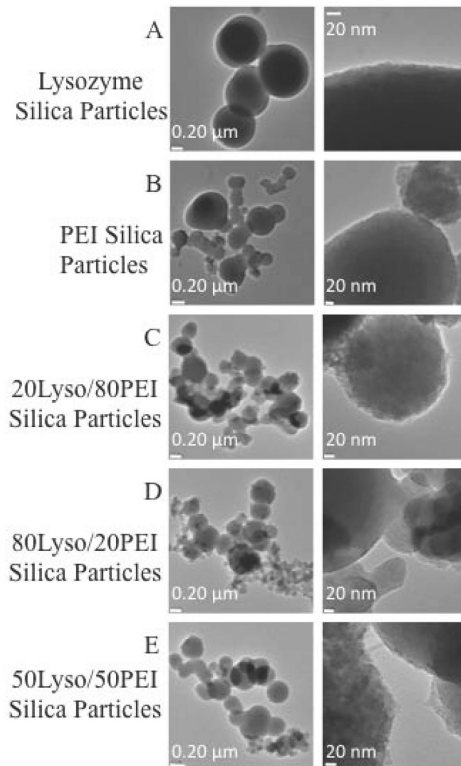


**Figure 3.** TEM images of the hCE1 encapsulated silica particles at two magnifications. Particles were air dried on a carbon stabilized copper grid prior to imaging.

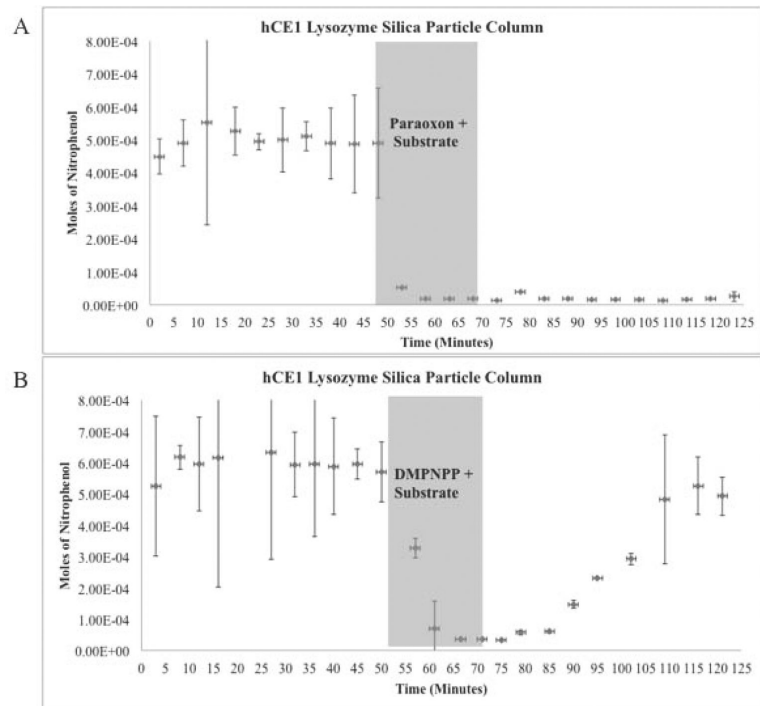


**Figure 4.** Microbore columns packed with lysozyme catalyzed silica particles containing hCE1 at a concentration of  $8.065 \times 10^{-2}$  nmol used to detect pesticides. The columns were equilibrated at 25° C to maximum activity with 5 mM substrate before 1 mM pesticide was applied (grey box). The eluent from the column was collected and measured in triplicate at the respective time points. All data points had an N = 3 and S.E. is reported.

**Table I**

hCE1 rate of pNBP hydrolysis in solution compared to silica particles created with different catalysts.

Sample	hCE1 Activity (moles of nitrophenol/second)	R <sup>2</sup>
hCE1 in solution	$3.42 \times 10^{-7}$	0.99
Lysozyme	$2.74 \times 10^{-7}$	0.99
R5	$2.90 \times 10^{-7}$	0.99
PEI	NA	
80% Lysozyme, 20% PEI	$2.52 \times 10^{-7}$	0.99
50% Lysozyme, 50% PEI	$3.03 \times 10^{-8}$	0.99
20% Lysozyme, 80% PEI	NA	
Lysozyme washed with 1% Tween 20	$1.50 \times 10^{-7}$	0.99
hCE1 Solution with 1% Tween 20	$6.04 \times 10^{-8}$	0.99

NA: not applicable, no enzyme activity contained in the particles.

**Table II**

Kinetic parameters for the metabolism of pNPB by hCE1 in solution and in lysozyme catalyzed silica particles.

Kinetic Parameters	hCE1 in Solution	hCE1 in Lysozyme Silica
$K_m$ (mM)	$3.30 \pm 0.44$	$10.13 \pm 0.85$
$V_{max}$ ( $\mu\text{mole}/\text{min}/\text{mg}$ )	$97.71 \pm 4.84$	$189.72 \pm 7.41$
Curve Fit ( $r^2$ )	0.99	0.99
$k_{cat}/K_m$ ( $\text{s}^{-1} \text{M}^{-1}$ )	$6.09 \times 10^4$	$3.85 \times 10^4$

N=3, S.E. for  $K_m$  and  $V_{max}$  values